

Rate Constant for the Reaction of O(³P) with Pyridine from 323 to 473 K

F. L. Tabarés and A. González Ureña*

Departamento de Química Física, Facultad de Química, Universidad Complutense de Madrid, Madrid—3, Spain
(Received: November 29, 1982)

Reactive mixtures O(³P) plus pyridine were produced and studied in our fast-flow discharge apparatus. Several chemiluminescent radiations were identified as the electronic transitions CH(A²Δ-X²Π), OH(AΣ⁺-X²Π), and CN(B²Σ⁺-X²Σ⁺) and their band intensities recorded as a function of the pyridine concentration. By using pseudo-first-order conditions we measured the rate constant for the initial reaction via the chemiluminescent detection of oxygen atoms with NO. Over the temperature range of 323-473 K the measured rate constants are well represented by the Arrhenius expression: $k/(\text{cm}^3 \text{mol}^{-1} \text{s}^{-1}) = [(2.9 \pm 0.3) \times 10^{12}] \exp[-2500 \pm 300/RT]$. A comparison with the analogous O + benzene reaction is made including some comments on the electrophilic attack of both aromatic rings by the oxygen atom.

Introduction

The reactions of organic nitrogen compounds with ground-state oxygen atoms are of interest not only because of their intrinsic importance in chemical kinetics, but because of practical applications to environmental problems, i.e., combustion processes, atmospheric chemistry, and photochemical air pollution.

As far as we are aware, there has not been until now a single determination of the Arrhenius parameters for the reaction of atomic oxygen with pyridine and its derivatives and only the rate constant at 298 K has been determined by Mani and Sauer¹ via the fast-flow technique. On the other hand, the analogous reaction of atomic oxygen and benzene has been studied by a variety of techniques² and, more recently, in a previous paper³ the CH(A²Δ-X²Π) and OH(A²Σ⁺-X²Π) chemiluminescent radiations from O(³P) + C₆H₆ reactive mixtures have been reported and monitored as a function of reactant concentration for several temperatures. Therefore, we have undertaken a systematic investigation of these aromatic (heterocyclic) compounds plus oxygen reactions and in the present paper the rate constants for the O(³P) + pyridine reaction over the temperature range of 323-473 K are reported. The analysis and comparison of the present vs. previous benzene reaction data provide us an excellent opportunity to understand the details and mechanism of the aromatic ring attack by the O(³P) atom and the major effect that one would expect in such molecular mechanism when a carbon atom (in the aromatic ring) is changed by a different atom, a nitrogen atom in the present case.

As described below the O + pyridine rate constant values here reported were obtained via the fast-flow technique monitoring at a given reaction time either the product or reactant chemiluminescence as a function of concentration and temperature. Product CH*, OH*, and CN* chemiluminescence was observed and, on the other hand, the oxygen atom concentration was followed by the NO + O + M → NO₂* + M chemiluminescent reaction.

(1) Mani, I.; Sauer, M. C., Jr. *Adv. Chem. Ser.* 1968, No. 82, 142.
(2) (a) Bocoock, G.; Cvetanovic, R. J. *Can. J. Chem.* 1961, 39, 2436. (b) Grovenstein, E., Jr.; Mosher, A. J. *J. Am. Chem. Soc.* 1970, 92, 3810. (c) Mani, I.; Sauer, M. C., Jr. *Adv. Chem. Ser.* 1968, No. 82, 142. (d) Avramenko, L. I.; Kolesnikova, R. V.; Savinova, G. I. *Izv. Akad. Nauk SSSR, Ser. Khim.* 1965, 1, 28. (e) Bonano, R. A.; Kin, P.; Lee, J. H.; Timmons, R. B., *J. Chem. Phys.* 1972, 57, 1377. (f) Furuyama, D.; Ebara, N. *Int. J. Chem. Kinet.* 1975, 7, 289. (g) Colussi, A. J.; Singleton, D. L.; Irwin, R. S.; Cvetanovic, R. J. *J. Phys. Chem.* 1975, 79, 1900. (h) Atkinson, R.; Pitts, J. N., Jr. *Chem. Phys. Lett.* 1979, 63, 485. (i) Sloane, T. M. *J. Chem. Phys.* 1977, 67, 2267.

(3) Tabares, F.; Sáez Rabanos, V.; González Ureña, A. *J. Chem. Soc., Faraday Trans. 1* 1982, 78, 3679-89 and references cited therein.

TABLE I

Experimental Conditions			
gas flow, μmol s ⁻¹			
Ar			1300
N ₂ O			200
O ₂			140
C ₅ H ₅ N			5.5-25.0
total press., torr			
			2.0
discharge frequency, Hz			
			42.5
discharge power, W			
			100
reaction time, ms			
			6.0 ^a
photomultiplier voltage, V			
			1800
typical signal, μV			
			2 × 10 ⁻³ -2 × 10 ⁻²
typical noise, μV			
			2 × 10 ⁻⁴
monochromator resolution, nm			
			4
flow velocity, cm s ⁻¹			
			4000
band intensities			
CH	A ² Δ-X ² π	4315	1.000
CN	B ² Σ ⁺ -X ² Σ ⁺	3883	0.65
OH	A ² Σ-X ² π	3090	0.25

^a Obtained by the time-of-flight method reported in ref 3.

Experimental Section

The experimental apparatus has been described elsewhere³ and briefly it consists of a (modulated) discharge fast-flow reactor where a reactive mixture of oxygen atoms and organic compounds is produced. The reaction extent is studied by monitoring the chemiluminescent radiation, properly detected at the observation zone, from (a) any chemiluminescent product, if it is formed, or (b) NO₂* chemiluminescence emission from the NO + O + M → NO₂* + M reaction due to the residual O atom concentration. As described in detail in ref 3, oxygen atoms in the present experiment are produced by modulated discharge (microwave unit Electromedical Supplies, Microtom 200 MK2) and any product emission would appear modulated at the same frequency as the discharge does. Therefore, a preamplifier/lock-in amplifier system detection (Keithley Models 427/840) at the output of our photomultiplier would increase our signal-to-noise ratio until a factor of 100 (see Table II) making possible kinetics and/or spectroscopic studies of weak chemiluminescence emissions present in these highly reactive systems.

Table I illustrates the present experimental conditions. During our experiments the O atoms were produced by microwave discharge of either Ar/O₂ or Ar/N₂O. The latter was used to obtain the rate constant and Arrhenius parameters of the O + pyridine reaction by monitoring at 6.0 ms of reaction time the residual NO₂ emission intensity

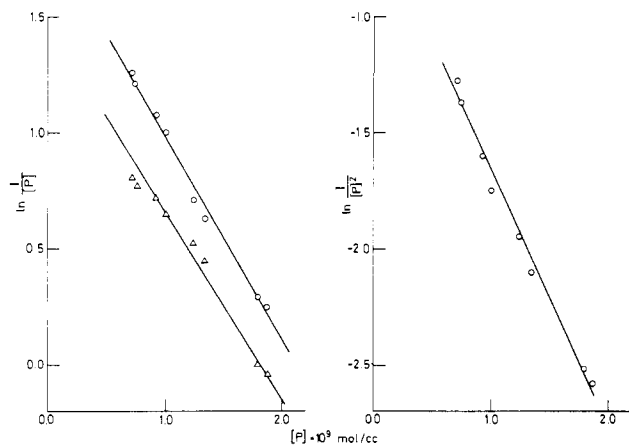


Figure 1. logarithmic representation of the several emissions observed in the O + pyridine reaction. Left: (circles) CH emission; (triangles) CN emission. Right: OH emission. Ordinate: log plot of the intensity divided by pyridine concentration (linear or square). Abscissa: pyridine concentration.

(produced in the initial Ar/N₂O discharge) as a function of the pyridine concentration and reactant temperature. To avoid condensation and because of the low pyridine vapor pressure the reactant storage vessel including the needle valve was introduced from a (heated) bath whose temperature was monitored by means of a thermocouple located inside of the vessel. Baths at different temperatures, were used to change the reactant vapor pressure and then its flow under the same fixed valve position. To calibrate the pyridine flow the same procedure was repeated as in using benzene. The drop of the liquid level in a Pyrex tube (of a constant cross section) was measured as a function of time and at the same temperature and needle valve position.

All the gases were from Sociedad Española del Oxígeno of a purity of 99.9% and were used directly. Pyridine and benzene (Merck purity 99.5%) were purified by low-temperature distillation and subsequent degassing at 77 K. Flow velocity determination was carried out by the time-of-flight technique as described previously.³

Results

Observed Emissions and Pyridine Concentration Dependence at Given Initial Conditions. Table II summarizes several emission bands identified and recorded when reactive mixtures of O(³P) + pyridine were prepared via the Ar/O₂ discharge. The observed band intensities, corrected for the instrument's response, were normalized with the intensity of the 4315-Å band of CH(A²Δ-X²Π) taken as unity. Note that the present emissions resemble those observed in the case of the O(³P) + C₆H₆ mixture case with the important difference that the CN-(B²Σ⁺-X²Σ⁺) is now present.

As in previous studies, it was found^{3,4} that these emission intensities change with reactant concentration and temperature. Such experimental dependence for a given temperature of 360 K is displayed in Figure 1 at a fixed initial concentration of oxygen atoms. These data are well represented by the following empirical relations

$$I(\text{CH}^*) = a_1[\text{P}] \exp(-b_1[\text{P}]) \quad (1)$$

$$I(\text{CN}^*) = a_2[\text{P}] \exp(-b_2[\text{P}]) \quad (2)$$

$$I(\text{OH}^*) = a_3[\text{P}]^2 \exp(-b_3[\text{P}]) \quad (3)$$

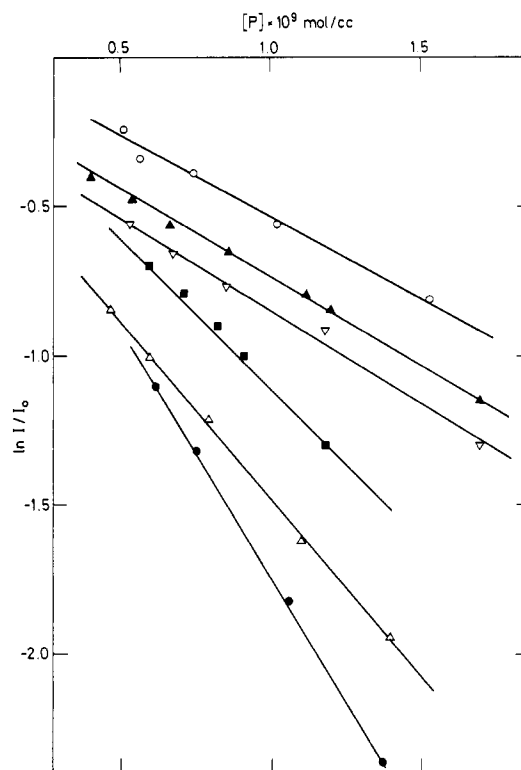


Figure 2. Logarithmic representation of the NO₂* emission intensity normalized with the residual intensity I_0 , i.e., in absence of pyridine vs. the pyridine concentration for several temperatures: (O) 323, (▲) 328, (▽) 360, (■) 388, (Δ) 432, (●) 473 K. The solid lines are straight lines through the data.

where [P] is the pyridine concentration and a_i and b_i ($i = 1, 2, 3$) are parameters depending on temperature but not on pyridine concentration.

Rate Constant Parameters from the Residual O Atoms Titration. As indicated before the Ar/N₂O discharge produces substantial NO + O products to give an intense NO₂* glow from the NO + O + M → NO₂* + M chemiluminescent reaction. Under these circumstances it is possible to determine the O + organic compound → products rate constant merely by monitoring the NO₂* emission intensity at a given reaction time, i.e., fixed downstream position and a wavelength of $\lambda = 550$ nm providing that the following conditions exist: (a) The organic compound reactivity with NO is much less than with O and therefore the NO concentration does not change substantially upon reaction with the organic reactant during the 6 ms that is required for the reactants to reach the observation zone. Experiments were done either introducing the NO at the observation zone (i.e., letting it take part in the reaction for less than 1 ms) or forming it in the discharge of the N₂O at the beginning of the reaction. In both cases the obtained rate constant values were found to be the same within a range of 8–10%, i.e., the experimental error of the present technique, even though one may expect different [O]₀ from these two methods. Moreover, several runs were carried out by changing the N₂O/Ar ratio in the discharge. The same slope in the Figure 2 representation (see below) was always obtained. This is an indication that our data were obtained in pseudo-first-order conditions under which [O] will follow a typical exponential decay. (b) Since a termolecular mechanism may play an important role in the above reaction, care must be taken to hold [M] in excess of the reactant concentration to prevent any emission intensity changes due to variation in [M] which may be caused by changes in the organic compound concentration. All these

TABLE II: Arrhenius Equations and Resonance Energy of the O + X → Products Reactions with X = Benzene, Pyridine

Arrhenius eq	X = benzene	X = pyridine
$k, \text{cm}^3 \text{mol}^{-1} \text{s}^{-1}$	$[(1.5 \pm 0.6) \times 10^{14}] \exp[(-4400 \pm 500)/RT]^a$ $[(2.8 \pm 0.4) \times 10^{13}] \exp[(-4940 \pm 160)/RT]^b$ $[(6.7 \pm 0.7) \times 10^{13}] \exp[(-4000 \pm 300)/RT]^c$	$[(2.9 \pm 0.3) \times 10^{12}] \exp[(-2500 \pm 300)/RT]^d$
$\beta, e \text{ kcal mol}^{-1}$	36.1	22.7

^a From ref 5 (ESR data). ^b From ref 8. ^c Present and ref 3 results. ^d Present results. ^e Resonance energy of X.

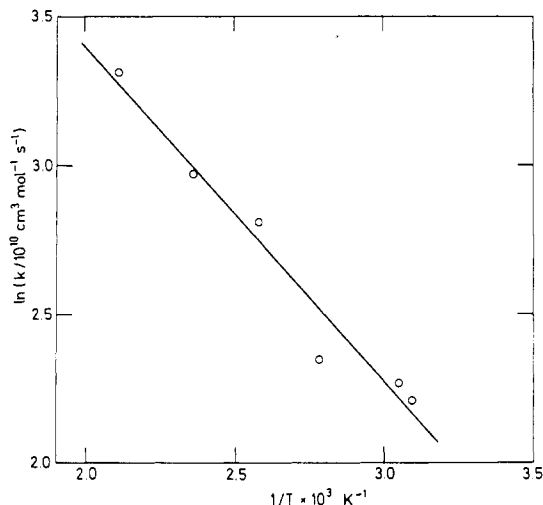


Figure 3. Arrhenius plot for the O plus pyridine reaction. Circles: present experimental values (see Table II). Solid line: least-squares fit.

conditions were maintained during our experiments and several runs of the well-known O(³P) + C₆H₆ reaction were carried out to test our procedure. The NO₂* emission at $\lambda = 550 \text{ nm}$ was monitored for several temperatures as a function of C₆H₆ concentration. In this case and using the pseudo-first-order approximation one obtains

$$I_{\text{NO}_2^*} \sim [\text{NO}][\text{O}] = [\text{NO}][\text{O}_0] \exp\{-kt[\text{X}]\}$$

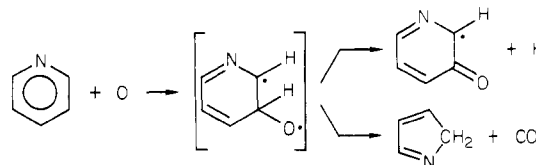
where [X] is the benzene or pyridine concentration, [O]₀ and [O] are the initial and actual oxygen atom concentrations, and k and t are the total oxygen atom consumption rate constant and the reaction time, respectively. A plot of $\log I_{\text{NO}_2^*}$ vs. [X] should give a straight line of slope $-kt$, i.e., total rate constant times the reaction time. As an example Figure 2 shows this type of representation for the pyridine reaction at several temperatures. The $I_{\text{NO}_2^*}$ emission intensities were reduced with $I_{\text{NO}_2^*}^0$, i.e., the intensity in the absence of X, and a plot of $\log I_{\text{NO}_2^*}/I_{\text{NO}_2^*}^0$ vs. [X] is displayed. Once the reaction time is known, one can get the experimental k values. Table II lists the actual benzene and pyridine rate constant values so obtained. An Arrhenius plot for the pyridine reaction is shown in Figure 3 from which a value of $E_a = 2.5 \pm 0.3 \text{ kcal/mol}$ was obtained. Our experimental activation energy for the O + benzene reaction of $E_a = 4.0 \pm 0.3 \text{ kcal/mol}$ in good agreement with the literature value⁵ and our previous determination by the chemiluminescent method³ provides consistency for the pyridine plus oxygen activation energy. Over the temperature range of 323–473 K the measured rate constants are well represented by the expression

$$k = [(2.9 \pm 0.3) \times 10^{12}] \exp[-(2500 \pm 300)/RT] \text{ cm}^3 \text{ mol}^{-1} \text{ s}^{-1}$$

Discussion

The present study of the O(³P) + pyridine reaction including both rate data and the observed emissions deserves some comments particularly when compared with the analogous O(³P) + benzene reaction reported in our previous study, as indicated.

First of all, as displayed in Table II, the smaller room-temperature rate constant value of the pyridine vs. the benzene reaction can be explained in terms of the different resonance energies of both aromatic rings. Obviously the nitrogen atom has a negative inductive effect, which withdraws electrons of the aromatic ring decreasing the resonance energy and directing the oxygen attack to the meta positions and, therefore, reducing the "steric factor" with respect to the benzene case. This mechanism (i.e., the preferred attack to the meta position) would be consistent with the absence (or low yield) of NO and CNO emissions as observed. Thus, by analogy with the benzene case⁶ one can write as the first two reaction pathways:



It seems that to form this biradical "transition-state" configuration a lower activation energy is required due to the initial relative activation of the pyridine vs. benzene associated with the loss of resonance energy from the introduced heteroatom. Moreover, since the lower the resonance energy the more localized is the electron density within the molecule, one may also expect lower reactivity for the pyridine than for the benzene with the oxygen atom because of the electrophilic nature of the attack. This factor can contribute to explain the low preexponential ratio of both reactions; i.e., from Table II one obtains $A(\text{pyridine})/A(\text{benzene}) = 0.020\text{--}0.10$. This observed ratio is smaller than one might expect even after allowance for the statistical difference in the preferred meta attack in the pyridine vs. benzene reaction (i.e., $2/6 = 0.33$). From Table II one can obtain an $A(\text{pyridine})/A(\text{benzene})$ ratio of 0.04 under our same experimental conditions. Considering the statistical difference (in the ring attack) of $2/6 = 0.33$ a stoichiometric factor ratio of $0.04/0.33 = 0.12$ would be necessary which seems too low considering the overall similarity of these two (aromatic rings) fast reactions with probably the same type of complex (radical) reactions under identical experimental conditions. Thus, one may consider that the electron density localization around the nitrogen atom not only decreases the activation energy but also reduces the "reaction size", the actual reaction cross section, in a simply geometrical collision representation of the reactive event.

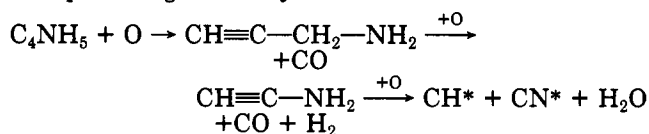
To explain qualitatively the simultaneous observation of CN* and CH* emissions one can consider that the C₄NH₅ diene, described in the above scheme, can probably follow a similar reaction sequence as the cyclopentadiene⁷

(5) Bonano, R. A.; Kin, P.; Lee, J. H.; Timmons, R. B. *J. Chem. Phys.* 1972, 57, 1377.

(6) Sibener, S. J.; Buss, R. J.; Casavecchia, P.; Hirooka, T.; Lee, Y. T. *J. Chem. Phys.* 1980, 72, 4341.

(7) Nakaruma, K.; Koda, S. *Int. J. Chem. Kinet.* 1979, 9, 67.

does producing secondary and radical reactions as follows:



Of course, a detailed mechanism of these complex reactions would perhaps require not only more experimental work, but also a different experimental technique mainly

(8) Nicovich, J. M.; Gump, C. A.; Ravishankara, A. R. *J. Phys. Chem.* 1982, 86, 1684.

directed toward identifying those intermediates or precursors present in our system. At the moment our main goal was to report the main experimental findings and to relate them with the basic chemical structure of the reactant aromatic rings. In this direction work is in progress with thiophene and other heterocyclics in our laboratory.

Acknowledgment. This work received financial support from the Comision Asesora of Spain.

Registry No. Pyridine, 110-86-1; atomic oxygen, 17778-80-2.

Gas Absorption with Instantaneous Chemical Reaction. Absorption of Sulfur Dioxide by Aqueous Sodium Bisulfite

D. G. Lealst

Department of Chemistry, University of Western Ontario, London, Ontario, Canada N6A 5B7 (Received: December 9, 1982)

Equations are derived for estimating rates of absorption of gas by ternary absorbents. For semiinfinite, convection-free absorbents, the rate of absorption equals $\Delta c_1(D_a/\pi t)^{1/2}$ where Δc_1 is the quantity of gas required to saturate a unit volume of bulk absorbent to the partial pressure of gas at the surface of the absorbent, D_a is an apparent diffusion coefficient defined in terms of ternary diffusion coefficients in the absorbent, and t is the time. This result applies to absorption by chemically inert systems, and to absorption with simultaneous chemical reaction provided the reaction rates are sufficiently rapid to effectively guarantee local chemical equilibrium. For purposes of illustration, absorption of sulfur dioxide by aqueous solutions of sodium bisulfite is discussed. In this system ternary diffusion of the partially hydrolyzed dissolved gas yields a concentration-dependent apparent diffusion coefficient that varies between 1.5×10^{-9} and $8.5 \times 10^{-9} \text{ m}^2 \text{ s}^{-1}$ at 20 °C.

Introduction

Efficient gas absorption often depends on chemical reaction of the dissolved gas with an involatile component in the absorbent. Reaction of oxygen with hemoglobin, for example, plays a key role in respiratory processes. In the chemical industry, aqueous solutions of acids or bases are widely used to absorb gases such as ammonia, carbon dioxide, hydrogen sulfide, and sulfur dioxide. So that the rate of absorption with reaction can be estimated,¹⁻⁶ it is common practice to assume that diffusion in the absorbent is pseudobinary. In real systems, however, the solute fluxes are coupled by nonideal thermodynamic behavior and by chemical reaction.^{7,8} With absorption processes involving electrolytes, there is the additional complication that fluxes of ions are coupled to each other by the electric field they produce, even at very low concentrations.^{9,10} Very large

departures from pseudobinary behavior are likely whenever diffusivities of the various species are widely different.⁹⁻¹⁴

How is gas absorption influenced by multicomponent diffusion in the absorbent? To answer this question, we derive equations to describe absorption with ternary diffusion in the absorbent. For purposes of illustration, absorption of sulfur dioxide by aqueous sodium bisulfite is discussed in detail. This system was chosen for several reasons. First, data¹⁵⁻²³ are available to make reliable estimates of the appropriate ternary diffusion coefficients. Second, absorption of sulfur dioxide by aqueous solutions is of importance to pollution studies. And finally, the recent report²⁴ that the ternary diffusivity of acetic acid

- (1) Danckwerts, P. V. *Trans. Faraday Soc.* 1951, 47, 1014.
- (2) Danckwerts, P. V. *Ind. Eng. Chem.* 1951, 43, 1460.
- (3) Sherwood, T. K.; Pigford, R. L. "Absorption and Extraction"; McGraw-Hill: New York, 1952; p 332 and Chapter 9.
- (4) Crank, J. "The Mathematics of Diffusion"; Oxford University Press: London, 1956; p 124.
- (5) Bird, R. B.; Stewart, W. E.; Lightfoot, E. N. "Transport Phenomena"; Wiley: New York, 1960; p 599.
- (6) Danckwerts, P. V. *Chem. Eng. Sci.* 1968, 23, 1045.
- (7) Vitagliano, V. *J. Phys. Chem.* 1970, 74, 2949.
- (8) Wendt, R. P. *J. Phys. Chem.* 1965, 69, 1227.
- (9) Lealst, D. G.; Lyons, P. A. *Aust. J. Chem.* 1980, 33, 1869.

- (10) Lealst, D. G. *J. Chem. Soc., Faraday Trans. 1* 1982, 78, 3069.
- (11) Revzin, A. *J. Phys. Chem.* 1972, 76, 3419.
- (12) Kim, H.; Reinfelds, G.; Costing, L. *J. Phys. Chem.* 1973, 77, 934.
- (13) Lealst, D. G.; Lyons, P. A. *J. Phys. Chem.* 1982, 86, 564.
- (14) Lealst, D. G. *Chem. Eng. Sci.*, submitted for publication.
- (15) Campbell, W. B.; Maass, O. *Can. J. Res.* 1930, 2, 42.
- (16) Morgan, O. M.; Maass, O. *Can. J. Res.* 1931, 5, 162.
- (17) Eriksen, T. *Chem. Eng. Sci.* 1967, 22, 727.
- (18) Robinson, R. A.; Stokes, R. H. "Electrolyte Solutions", 2nd ed; Academic Press: New York, 1959; Appendix 6.2.
- (19) Whitney, R. P.; Vivian, J. E. *Chem. Eng. Progr.* 1949, 45, 323.
- (20) Groothuis, H.; Kramers, H. *Chem. Eng. Sci.* 1955, 4, 17.
- (21) Lynn, S.; Straatemeier, J. R.; Kramers, H. *Chem. Eng. Sci.* 1955, 4, 49.
- (22) Toor, H. L.; Chiang, S. H. *AIChE J.* 1959, 5, 339.
- (23) Johnstone, H. F.; Leppla, P. W. *J. Am. Chem. Soc.* 1934, 56, 2233.
- (24) Lealst, D. G.; Lyons, P. A. *J. Phys. Chem.* 1981, 85, 1756.